Research Article **Open Access**

Ilona Iatcheva*, Denitsa Darzhanova, and Marina Manilova

Modeling of electric and heat processes in spot resistance welding of cross-wire steel bars

https://doi.org/10.1515/phys-2018-0001
Received November 2, 2017; accepted November 30, 2017

Abstract: The aim of this work is the modeling of coupled electric and heat processes in a system for spot resistance welding of cross-wire reinforced steel bars. The real system geometry, dependences of material properties on the temperature, and changes of contact resistance and released power during the welding process have been taken into account in the study.

The 3D analysis of the coupled AC electric and transient thermal field distributions is carried out using the finite element method. The novel feature is that the processes are modeled for several successive time stages, corresponding to the change of contact area, related contact resistance, and reduction of the released power, occurring simultaneously with the creation of contact between the workpieces. The values of contact resistance and power changes have been determined on the basis of preliminary experimental and theoretical investigations.

The obtained results present the electric and temperature field distributions in the system. Special attention has been paid to the temperature evolution at specified observation points and lines in the contact area. The obtained information could be useful for clarification of the complicated nature of interrelated electric, thermal, mechanical, and physicochemical welding processes. Adequate modeling is also an opportunity for proper control and improvement of the system.

Keywords: spot resistance welding; contact resistance; coupled electric and thermal field; 3D FEM modeling

PACS: 41.20.-q, 44.10.+i

1 Introduction

Spot resistance welding (SRW) has been known for a long time as very widely applicable in a variety of industrial areas where it is possible to automate the production process. The great technological advantages: high efficiency, precision and simplicity [1–5] of SRW makes it very attractive and especially widespread in the automobile manufacturing industry, in robotic assembly lines, in some orthodontist clinics, in battery production, etc. The considerable and sustained interest in this type of welding is due to the exclusive feature of the method to inject a large amount of energy exactly into the zone specified for welding in a very short time interval (milliseconds), without excessive heating of the rest of the workpieces. The proper control of the processes, however, is particularly important and obligatory for its use in automated, high-tech production lines [6].

The subject of investigation in this work is a real system for spot resistance welding of reinforced steel bars. It is well known and also experimentally proved that quality of the welded joints depends on the preliminary selected combination of the main technological parameters – value and duration of the welding current and the contact pressure on the welded bars. The right choice of so called time-current combination (TCC) is an important factor that guarantees acceptable quality of the welded joints for specific diameters of the reinforced steels [7, 8]. A good opportunity for proper control of the behavior and improvement of the system efficiency is the detailed modeling of the processes in the SRW device, taking into account the whole complex of interrelated electric, thermal, mechanical and physicochemical processes and phenomena [9–11].

The aim of the work is precise analysis of the processes taking part in a system for contact resistance welding of cross-wire reinforced steel bars. As a starting point and a base for the studies, previous experimental [12] and theoretical [13, 14] investigations of the same system have been considered. The detailed 3D computer modeling of the coupled AC electric and transient thermal field distribution is carried out using the finite element method (FEM) and COMSOL Multiphysics 5.2 software package [15].

***Corresponding Author: Ilona Iatcheva:** Dept. of Theoretical Electrical Engineering, Technical University of Sofia, Sofia, 1000, Bulgaria, E-mail: iiach@tu-sofia.bg
Denitsa Darzhanova: Dept. Electrical Measurement Systems, Technical University of Sofia, Sofia, 1000, Bulgaria
Marina Manilova: Institute of Metal Science "Acad. A. Balevski", Bulgarian Academy of Sciences, Sofia, 1574, Bulgaria

The novelty of the study is that the electric and thermal field distributions in the welding region are modeled for several successive time stages of the welding process, corresponding to the change of contact spot area, related contact resistance and reduction of the released power.

2 Description of the investigated system

The welding principle of the studied system is illustrated in Figure 1. The system consists of two electrodes and two cross-wire steel bars. The two electrodes hold together with additional force the steel bars that are to be welded, while at the same time an alternating current is applied in the system for a short time. The large welding current concentrated into a small spot region causes release of a large amount of thermal power, proportional to the resistance between the electrodes. The contact area is heated by the released energy, which causes softening, melting, and bonding of the metals. Of specific importance is the fact that, because of the material softening, followed by melting and enlarging of the contact zone, the contact resistance and released power are significantly changed during the welding.

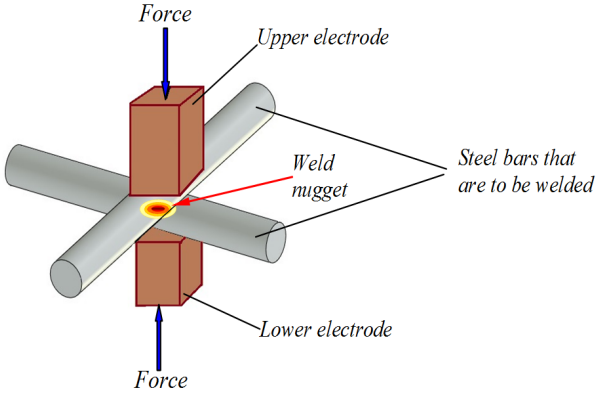

Figure 1: Principle scheme of the investigated system

The actual welding machine used for preliminary experiments [12] is shown in Figure 2. The system has been studied when 5–8 kA, 50 Hz AC current has been applied for 80 ms and the contact force is 500 N. The two welded bars are of 10mm diameter and the steel type is BSt500s (the melting point is about 1450°C). The melted contact zone diameters of successfully welded samples have been measured to be 4–5 mm (Figure 3).

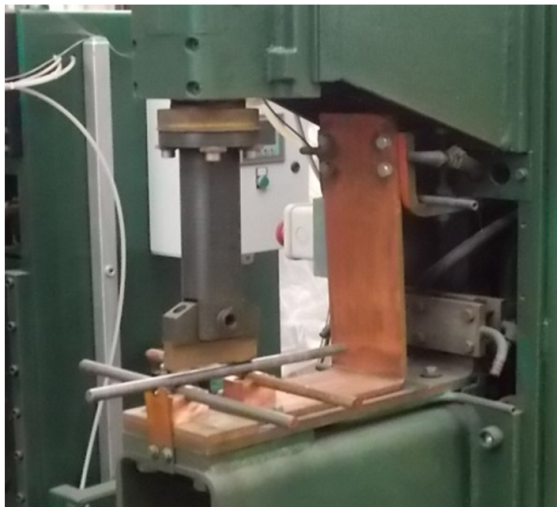

Figure 2: Welding machine used for preliminary experiments

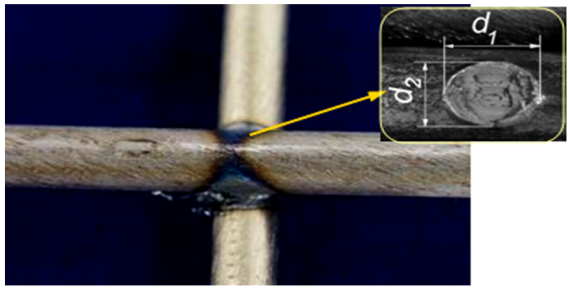

Figure 3: The melted contact zone diameters of successfully welded samples have been measured to be 4–5 mm

3 Mathematical formulation and basic points in numerical modeling

The processes taking part in the considered system are a complex of interrelated electric, thermal, mechanical and physicochemical phenomena. The present investigation is based on the analysis of coupled electric and thermal field distributions, studied for several successive time stages, corresponding to the change of contact spot area, related contact resistance, and reduction of the released power, occurring simultaneously with the creation of contact between the welded workpieces.

The mathematical formulation of the problem includes determination of the governing equations, boundary conditions, and the field sources corresponding to changes of the contact area dimensions, contact resistance, and released power, depending on the welding time.

3.1 Governing equations and boundary conditions

The modeling of the processes in the considered system is related to determination of coupled field distribution - AC electric field and transient thermal field.

The governing equations for the electric field are:

$$\begin{aligned} \nabla.\mathbf{J} &= 0 \\ \mathbf{J} &= \gamma\mathbf{E} + \mathbf{Je} \\ \mathbf{E} &= -\nabla V \end{aligned} \tag{1}$$

where **E** is the electric field strength, **J** is the current density, V is the scalar electric potential, and γ is the electric conductivity.

In order to take into account the specific changes in the contact spot area during the welding process, resulting in changes of the material state and properties, overlapping dimensions, and released power, a corresponding contact resistance has been introduced in the numerical modeling. The layer impedance and relevant overlapping are specified on the basis of preliminary experimental investigations [12], and boundary conditions have been introduced accordingly in the model with the given equations below [15]:

$$\begin{aligned} \mathbf{n}.\mathbf{J_1} &= \gamma_s(V_1 - V_2)/d_s \\ \mathbf{n}.\mathbf{J_2} &= \gamma_s(V_2 - V_1)/d_s \end{aligned} \tag{2}$$

The indices 1 and 2 refer to the two sides of the boundary, γ_s is the contact material conductivity, and d_s is layer thickness (overlapping).

The Ohmic losses determined in the electric field modeling

$$Q = J^2/\gamma, \tag{3}$$

are used in the coupled electric-thermal field modeling as a field source in the thermal field analysis.

The transient thermal field is modelled by the equation:

$$\rho C\partial T/\partial t + \nabla.(-k\nabla T) = Q \tag{4}$$

where T is the temperature, k is the thermal conductivity, ρ is the mass density, C is the heat capacity at constant pressure, and Q is the heat source, obtained using (3).

In the field modeling both convection and radiation boundary conditions have been taking into account:

$$-k\partial T/\partial n = h(T - T_{amb}) + \epsilon\sigma_{SB}(T^4 - T_{amb}^4) \tag{5}$$

where T_{amb} is the temperature far away from the modeled domain, h is the convection heat transfer coefficient, σ_{SB} is the Stefan-Boltzmann constant (5,67.10^{-8} Wm^{-2}K^{-4}), and ϵ is emissivity.

3.2 Determination of the field sources, corresponding to the contact area, contact resistance and released power

Determination of the field sources, corresponding to the contact area, contact resistance, and released power is based on the previous experimental [12] and theoretical [13] investigations. Although the theoretical approach (based on electrical analogy of heat transfer) was quite different from that used in the present work, the main assumptions about the dimensions of the affected contact region, corresponding contact resistance, and power change during the welding stages are accepted in the present study.

The driving source thermal power can be calculated as:

$$P(t) = R_C i^2(t), \tag{6}$$

where *i(t)* is the source current and R_C is the contact resistance between the two pressed samples. The average initial value for the contact resistance R_C was obtained via preliminary experimental investigations, but, as was noted, because of the material softening, followed by melting and enlarging of the contact zone, this resistance changes significantly. For simulation purposes, it was assumed that the contact resistance drops two times during the overall transient process at moments t_1 = 3 ms and t_2 = 30 ms. Therefore, the heat power released in the joint also changes its value twice in correspondence to the reducing resistance between the steel bars. Thus, the welding process has been considered (Figure 4) for three successive time stages: 0–0.003 s; 0.003–0.03s; 0.03–0.08s, related to the change of contact spot area, related contact resistance and reduction of the released power.

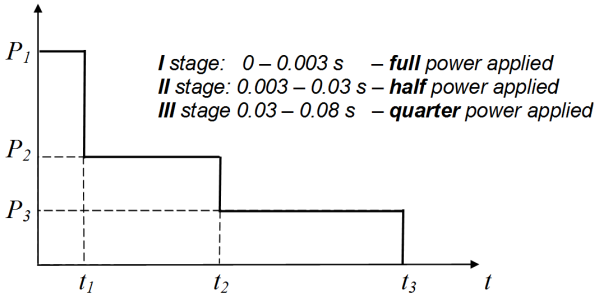

Figure 4: Three stages of welding process are considered, corresponding to the assumed three input power values

According to the described power changes, different welding currents have been considered in the modeling

for each of the three time stages. The current sources have been obtained as sinusoidal with amplitude determined correspondingly to the power of each stage (Figure 5).

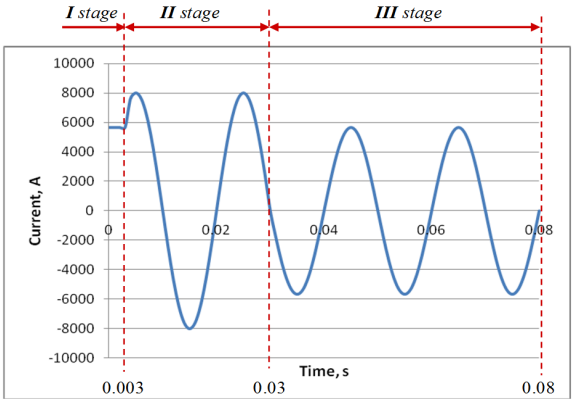

Figure 5: Current, applied in the FEM modeling, corresponding to the changes of the contact resistance and reduction of the released power during the welding

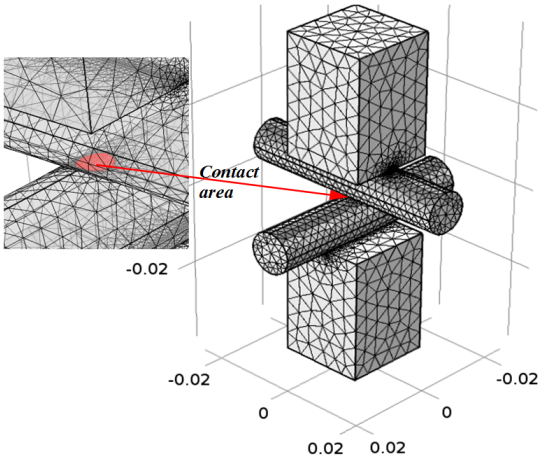

Figure 6: Finite element mesh in the studied area consists of 250 000 elements

4 FEM modeling and results

The transient coupled electric and thermal field problem was studied by the finite element method, using COMSOL Multiphysics 5.2 software package.

The FEM modeling of the electric and thermal field distribution during the welding process is carried out for the three stages, taking into account the real 3D geometry of the studied region and dependences of material properties on the temperature. The contact resistance determined on the basis of experimental and theoretical investigation of the system was has also been introduced in the FEM model.

4.1 FEM modeling of the system structure

The model of the system structure is illustrated with the 3D FE mesh of the studied area in Figure 6. The depth of overlapping in the presented structure is δ = 0.15 mm.

4.2 Electric field modeling

The electric field modeling is presented in the study by a map of electric potential distribution for three different RMS values of the applied in the modeling currents. As it was mentioned, the contact resistance changes significantly during the welding process and correct field analysis requires taking this into account. Therefore, special attention has been paid to the influence of the inclusion of contact resistance in the electric field modeling.

The influence of the contact resistance is very clearly seen and evaluated from comparison of electric potential distribution, presented in Figure 7 - field modeling without contact resistance and Figure 8 - field modeling with contact resistance in case of I = 7 kA. As it can be seen, the introduction of contact resistance leads to a significantly higher potential difference between the electrodes (2,5 times).

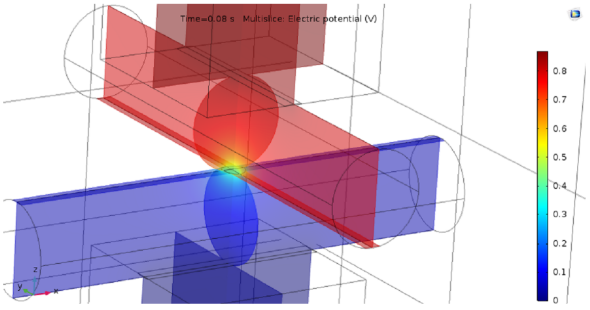

Figure 7: Distribution of the electric potential for I = 7 kA, overlapping δ = 0.15 mm (no contact resistance)

The influence of the applied current value is considered in the study by comparison of electric field distribution for three RMS values of the current. The results in case of overlapping δ = 0.15 mm are presented correspondingly

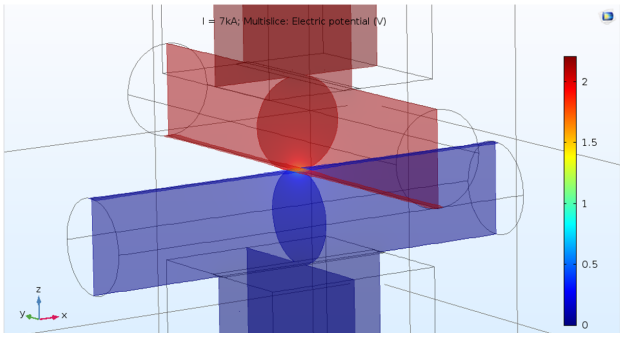

Figure 8: Distribution of the electric potential for I = 7 kA, overlapping δ = 0.15 mm (presence of contact resistance)

in Figure 8 for I = 7 kA; in Figure 9 for I = 5 kA; in Figure 10 for I = 9 kA.

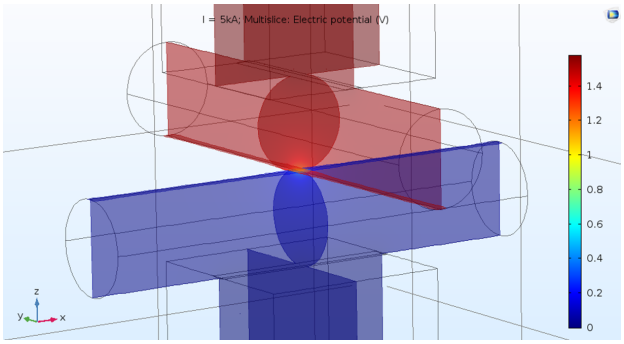

Figure 9: Distribution of the electric potential for I = 5 kA, overlapping δ = 0.15 mm (presence of contact resistance)

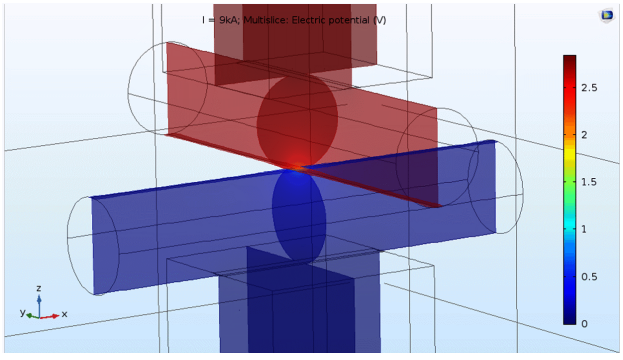

Figure 10: Distribution of the electric potential for I = 9 kA, overlapping δ = 0.15 mm (presence of contact resistance)

The comparison shows that as it can be expected the current increase reflects in the electric field potential increase.

4.3 Thermal field modeling

Special attention in the thermal field analysis has been paid to temperature in special observation areas (Figure 11). During the analysis the temperature has been monitored along the horizontal and vertical lines of the contact spot area and in points V_1, V_4 and V_8 (observed regions in [13]).

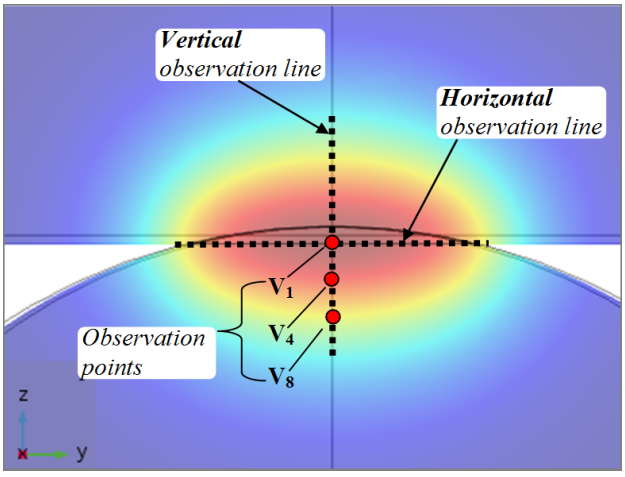

Figure 11: Location of the observation lines and points in the contact area

Evolution of the temperature during the first welding stage is illustrated in Figure 12, Figure 13 and Figure 14. The temperature distribution along the horizontal line of observation is presented in Figure 12, the temperature distribution along the vertical line of observation is presented in Figure 13, and the temperature change at the three observation points V_1, V_4 and V_8 for the period t = 0-0.003 s is shown in Figure 14.

The results of temperature field modeling show that in the second stage the temperature in the joint region reaches its maximum for the whole welding period. The temperature field distribution at the end of the second stage (t_2 = 30 ms) is illustrated in Figure 15.

Evolution of temperature during the second welding stage (t = 0.003 – 0.03 s) is illustrated correspondingly: in Figure 16 the temperature distribution along the horizontal line of observation, Figure 17 the temperature distribution along the vertical observation line and in Figure 18 the evolution of the temperature at the three observation points V_1, V_4 and V_8.

The results of the temperature field modeling in the third, last welding stage (t = 0.03 s – 0.08 s) are presented in Figures 19–22. The temperature field distribution at the

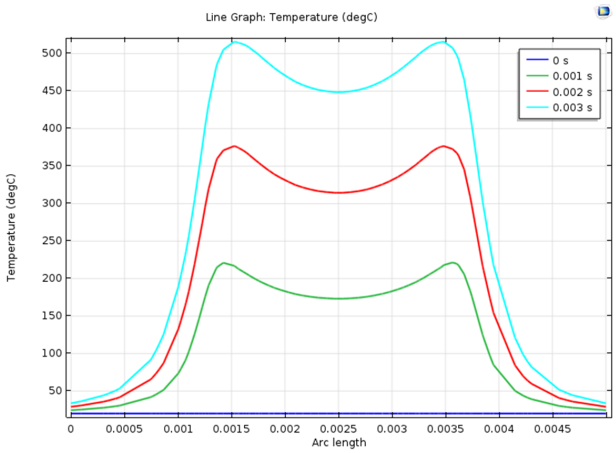

Figure 12: Evolution of the temperature distribution along the horizontal observation line during the first stage of welding (t = 0–0.003 s)

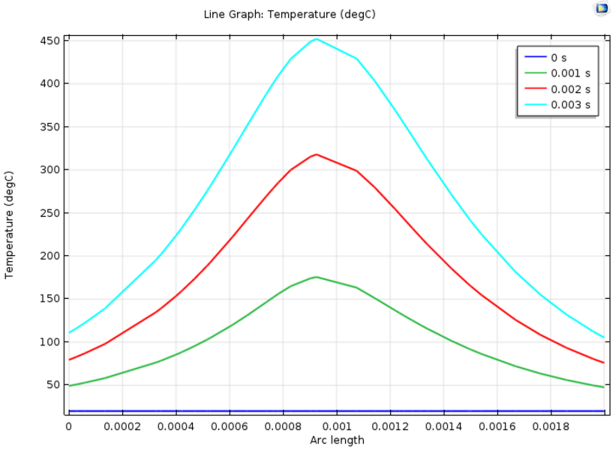

Figure 13: Evolution of the temperature distribution along the vertical observation line during the first stage of welding (t = 0–0.003 s)

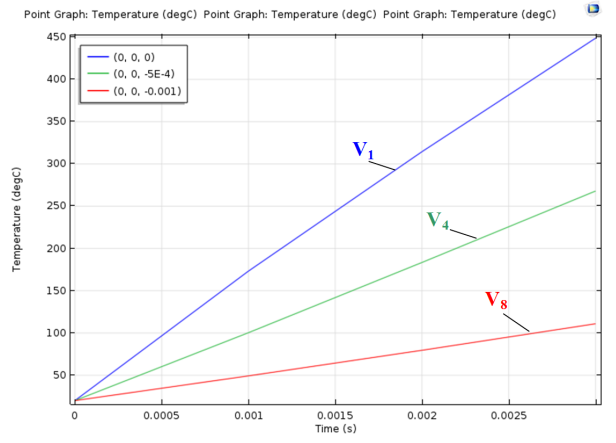

Figure 14: Evolution of the temperature at observation points V1, V4, and V8, during the first stage of welding (t = 0–0.003 s)

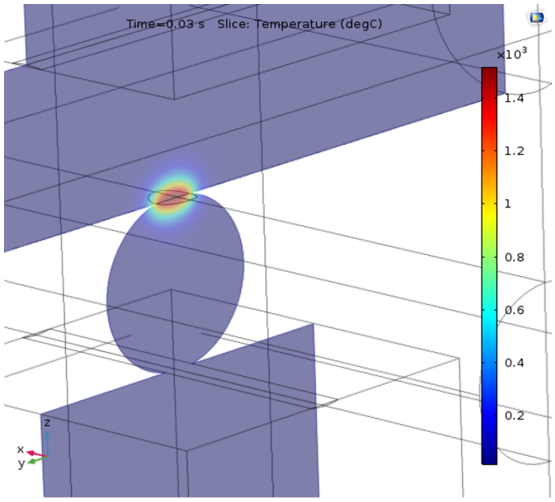

Figure 15: Temperature field distribution at the end of the second time stage after 30 ms treatment (when the temperature reaches its maximum for the whole welding period)

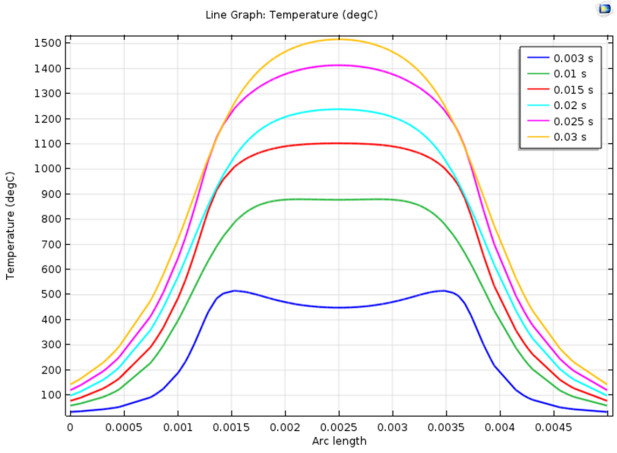

Figure 16: Evolution of the temperature distribution along the horizontal observation line during the second stage of welding (t = 0.003 s – 0.03 s)

end of the third stage (t_3 = 80 ms) has been illustrated in Figure 19.

The change of the temperature distribution along the horizontal observation line during the last welding stage (t = 0.03 s – 0.08 s) is shown in Figure 20, the temperature distribution along the vertical observation line is shown in Figure 21, and the temperature variation at the observation points V_1, V_4 and V_8 is shown in Figure 22.

The field analysis shows that compared with the temperature at the end of the second stage, there is some decrease in the temperature values in the center of the joint region during the last third welding stage. This can also be seen from the results shown in Figure 23, presenting the

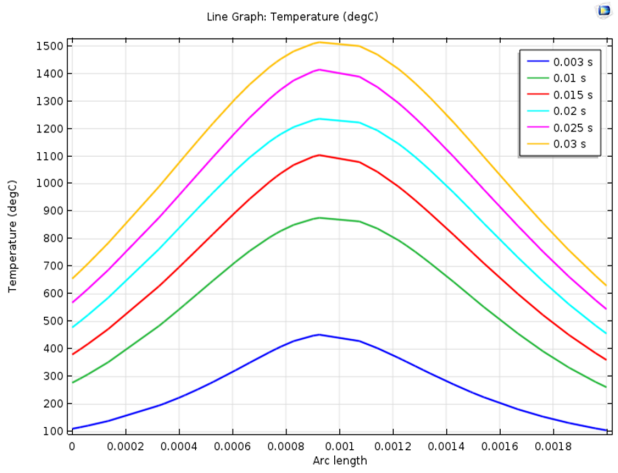

Figure 17: Evolution of the temperature distribution along the vertical observation line during the second stage of welding (t = 0.003 s – 0.03 s)

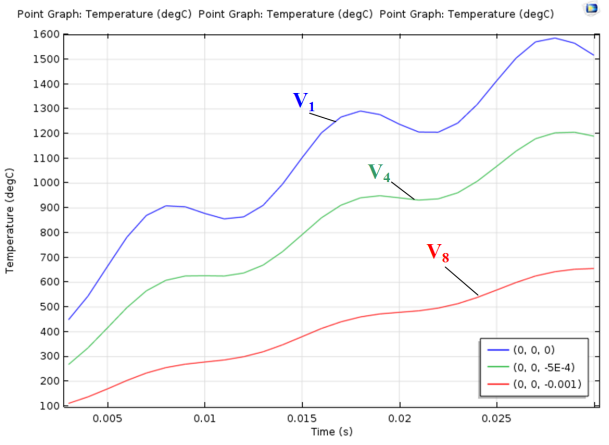

Figure 18: Evolution of the temperature in the observation points V1, V4 and V8, during the second stage of welding (t = 0.003 s – 0.03 s)

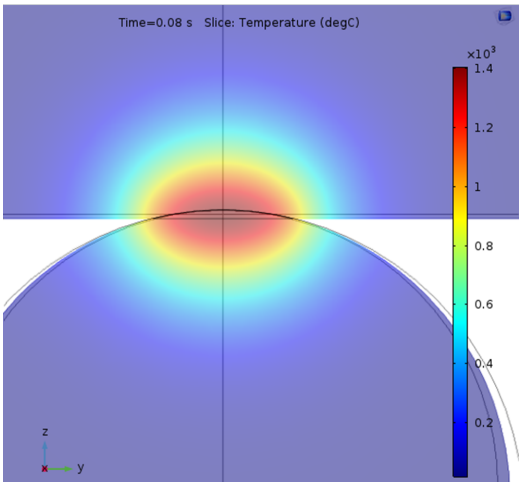

Figure 19: Temperature field distribution at the end of the last welding stage (after 80 ms treatment)

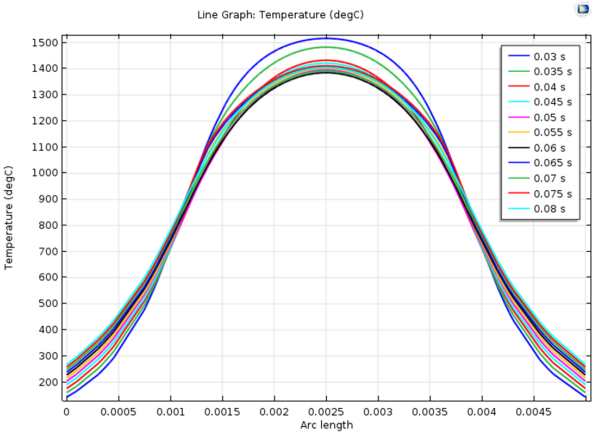

Figure 20: Evolution of the temperature distribution along the horizontal observation line during the last stage of the welding (t = 0.03 s – 0.08 s)

temperature changes at the observation points over the entire welding time.

5 Conclusion

Accurate 3D coupled electric and thermal field modeling of the spot resistance welding system has been carried out in the present work. The complex interrelated welding process have been studied using 3D FEM analysis, taking into account the real region geometry, material properties, dependencies, and changes of the contact resistance and the released power.

The novelty of the study is modeling of the processes for three, successive time stages of the welding process, corresponding to the change of contact spot area, related contact resistance, and reduction of the released power. Different welding currents have been applied in the FEM modeling for each of the three time stages. The current sources have been obtained as sinusoidal with amplitude, determined correspondingly to the released power of each stage.

The results have been obtained for the temperature distribution and its evolution in the contact area and specified observation lines and points. The analysis of the temperature distribution indicates that the desired temperature of 1450 C° has been reached in the experimentally determined dimensions of the contact spot area. This fact confirms the reliability of the proposed study, showing that scientific efforts are in the right direction. Further work can include taking into account the temperature dependence of the steel conductivity and the phase change.

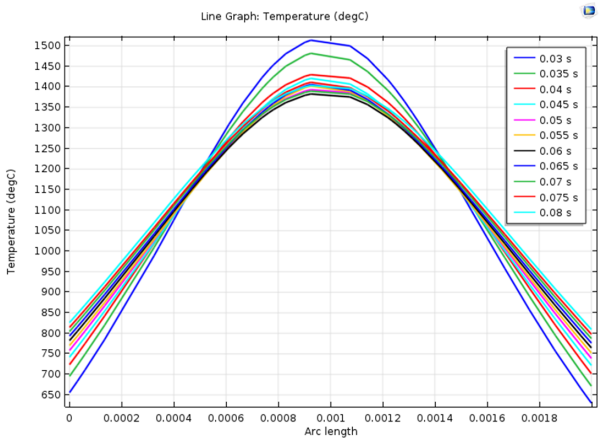

Figure 21: Evolution of the temperature distribution along the vertical observation line during the last stage of the welding (t = 0.03 s – 0.08 s)

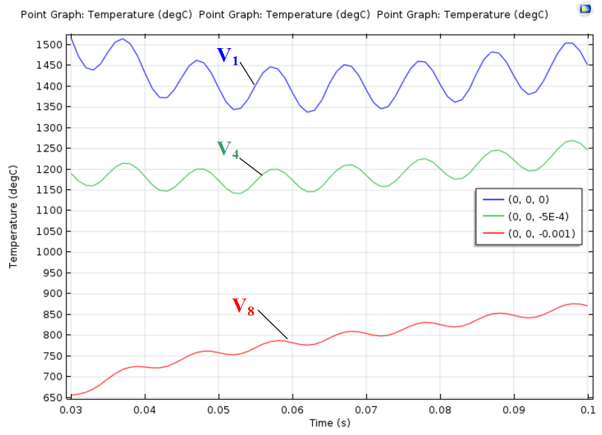

Figure 22: Evolution of the temperature at points of observation V1, V4 and V8, during the last stage of the welding (t = 0.03 s – 0.08 s)

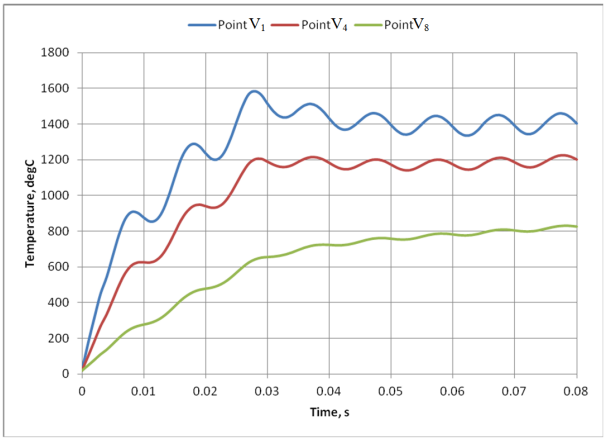

Figure 23: Evolution of the temperature at points of observation V1, V4 and V8, during the last stage of the welding (t = 0.03 s – 0.08 s)

The obtained information clarified the nature of complicated processes taking part during the welding and can also be used as a base for further optimization and improvement of the welding system.

Acknowledgement: The present work is supported by the National Science Fund of Bulgarian Ministry of Education and Science, Project DFNI E02-8/2014.

References

[1] Zhang H., Senkara J., Resistance welding, fundamentals and applications, CRC Press, 2006.

[2] Williams N. T., Parker J. D., Review of resistance spot welding of steel sheets. Part 1 Modelling and control of weld nugget formation, Int. Mater. Rev., 2004, 49(2), 45-75.

[3] Miller Electric Mfg. Co., Handbook for resistance spot welding, 2012-06, https://www.millerwelds.com/-/media/millerelectric/files/pdf/resources/bookspamphlets/resistance.pdf

[4] Holm R., Electric contacts, Inostrannaya literatura, Moscow, 1961, (In Russian)

[5] Scotchmer N., The other resistance process: crosswire welding, Weld. J., 2007, Dec., 36-39.

[6] Kulkarni A.S., Inamdar K.H., Effect of process parameters on resistance welding, J. Emerg. Technol. Innov. Res., 2015, 2(4), 963-967.

[7] Dennison A.V., Toncich D.J., Masood S., Control and process based optimisation of spot-welding in manufacturing systems, Int. J. Adv. Manuf. Technol., 1997, 13(4), 256-263.

[8] Hemmati M., Haeri M., Control of resistance spot welding using model predictive control, In Proc. 9th International Conference on Electrical and Electronics Engineering (2015, Bursa, Turkey), 864-868.

[9] Wyant R.A., Measurement and effect of contact resistance in spot welding, Electr. Eng., 1946, 65(1), 26-33.

[10] Wei P.S., Wu T.H., Electrical contact resistance effect on resistance spot welding, Int. J. Heat Mass Tran., 2012, 55(11-12), 3316-3324.

[11] Wei P.S.,Wu T.H., Effects of electrode contact condition on electrical dynamic resistance during resistance spot welding, Sci. Technol. Weld. Joining, 2014, 19(2), 173-180.

[12] Darzhanova D., Manilova M., Milanov K., Experimental study of the contact resistance of crossed cylindrical reinforcing steel bars, Electrotechnika & Electronica E+E, 2015, 50(5-6), 24-29.

[13] Darzhanova D., Iatcheva I.,Manilova M., Darjanov P., Simulation study of the heating process in contact resistance welding crossed steel bars, J. Mat. Sci. Technol., 2017, 25.

[14] Iatcheva I., Darzhanova D., Manilova M., Investigation of spot resistance welding system based on 3d field modeling using FEM, In Book of Abstracts, 18th International Symposium on Electromagnetic Fields in Mechatronics, Electrical and Electronic Engineering ISEF 2017 (14-16 September 2017, Lodz, Poland), 1-2.

[15] COMSOL, Inc., COMSOL Multiphisics user's guide, version 5.2, 2015.